Magnetic Resonance Imaging 79 (2021) 38–44

Contents lists available at ScienceDirect

Magnetic Resonance Imaging

journal homepage: www.elsevier.com/locate/mri

Age estimates from brain magnetic resonance images of children younger than two years of age using deep learning

Masahiro Kawaguchi [a], Hiroyuki Kidokoro [a,*], Rintaro Ito [b], Anna Shiraki [a], Takeshi Suzuki [a], Yuki Maki [a], Masaharu Tanaka [a], Yoko Sakaguchi [a], Hiroyuki Yamamoto [a], Yosiyuki Takahashi [a], Shinji Naganawa [c], Jun Natsume [a]

[a] Department of Pediatrics, Nagoya University Graduate School of Medicine, Nagoya, Japan
[b] Department of Innovative BioMedical Visualization, Nagoya University Graduate School of Medicine, Nagoya, Japan
[c] Department of Radiology, Nagoya University Graduate School of Medicine, Nagoya, Japan

ARTICLE INFO

Keywords:
Age estimation
Infant
Brain MRI
Deep learning
Convolutional neural network

ABSTRACT

The accuracy of brain age estimates from magnetic resonance (MR) images has improved with the advent of deep learning artificial intelligence (AI) models. However, most previous studies on predicting age emphasized aging from childhood to adulthood and old age, and few studies have focused on early brain development in children younger than 2 years of age. Here, we performed brain age estimates based on MR images in children younger than 2 years of age using deep learning. Our AI model, developed with one slice each of raw T1- and T2-weighted images from each subject, estimated brain age with a mean absolute error of 8.2 weeks (1.9 months). The estimates of our AI model were close to those of human specialists. The AI model also estimated the brain age of subjects with a myelination delay as significantly younger than the chronological age. These results indicate that the prediction accuracy of our AI model approached that of human specialists and that our simple method requiring less data and preprocessing facilitates a radiological assessment of brain development, such as monitoring maturational changes in myelination.

1. Introduction

Age estimates based on neuroimages are of clinical importance to understand normal and pathological brain development as well as aging [1]. Prediction accuracy has improved with the application of machine learning algorithms. For example, Franke et al. estimated brain age from adult brain magnetic resonance (MR) images using a machine learning algorithm based on relevance vector regression and reported that the overall mean absolute error (MAE) was 4.98 years [2]. Deep learning models based on convolutional neural networks (CNNs) further contribute to the progress of medical image analysis [3]. The innovation in deep learning for predicting brain age provides potential biomarkers for some neurodevelopmental and neurodegenerative disorders. However, most studies on predicting age have emphasized aging from childhood to adulthood and old age, and few studies have focused on early brain development in children younger than 2 years of age.

Infancy is an important period of brain development. Dynamic structural and functional developments during myelination from birth to 2 years of age have been revealed through brain MR images [4]. Gray matter (GM) displays a higher intensity on T1-weighted (T1w) images compared to white matter (WM) during the neonatal period, unlike in adulthood. The T1w intensity associated with the GM and WM becomes an adult pattern at approximately 11 months of age. By contrast, GM exhibits a lower T2-weighted (T2w) image intensity than does WM during the neonatal period. The T2w intensity contrast reverses as myelination progresses and becomes an adult pattern at approximately 18 months of age. Therefore, pediatric radiologists and pediatric neurologists can evaluate the progress of myelination and diagnose delayed myelination or congenital hypomyelination disorders based on a combination of T1w and T2w images. This is an important clinical indication for using deep learning to objectively estimate brain age in this age group.

Feasibility is an important consideration in medical artificial intelligence (AI). Various MR imaging data, including three-dimensional

* Corresponding author at: Department of Pediatrics, Nagoya University Graduate School of Medicine, 65 Tsurumai-cho, Showa-ku, Nagoya, Aichi 466-8550, Japan.
E-mail address: kidokoro@med.nagoya-u.ac.jp (H. Kidokoro).

https://doi.org/10.1016/j.mri.2021.03.004
Received 26 October 2020; Received in revised form 19 January 2021; Accepted 9 March 2021
Available online 12 March 2021

(3D) T1w MR images, diffusion tensor images, and resting-state functional MR data have been used to predict brain age. However, these images are not always available in the clinical setting. In addition, to extract features from those images, preprocessing with specific software is often required, and many tasks cannot be automated. Although advanced image acquisition and sophisticated preprocessing will likely lead to more accurate brain age predictions, a simple algorithm using raw MR image data with less preprocessing would allow clinicians to benefit from machine learning.

Here, we estimated brain age in children younger than 2 years of age with deep learning based on raw T1w and T2w MR image slices. Then, the accuracy was compared with that of human specialists. Furthermore, we estimated brain age with the deep learning model using MR images showing a significant myelination delay, thus validating the model output.

2. Materials and methods

2.1. Data acquisition

2.1.1. Dataset 1

In the present study, we used hospital-based MR imaging data, as there are few public brain MR image databases available for this population. We collected brain MR images of infants aged 0–24 months acquired in our Department of Pediatrics between April 2016 and March 2019. A total of 558 scans from 441 subjects were eligible for the study. These MR images were acquired for clinical purposes in infants who were suspected to have some brain abnormalities or who needed screening for central nervous system complications. In some patients, serial MR images were acquired at different ages and were treated as separate scans. One slice each of two-dimensional (2D) axial T1w and T2w images from each patient at the level of the corpus callosum splenium was used (Fig. 1A1 and A2). This is because the splenium and genu of the corpus callosum are indices of myelination, and because the axial slices contain extensive GM and WM areas. In our hospital, all axial images are acquired based on a reference straight line connecting the anterior commissure with the posterior commissure. The following scans were excluded: 1) scans lacking the required T1w and T2w sequences, 2) scans of infants born preterm (gestational age < 37 weeks), or born at an unknown gestational age, and 3) scans with abnormal findings or strong artifacts in the required slice. Abnormal findings included congenital and acquired brain abnormalities, such as destructive lesions due to hemorrhage, stroke, infectious and hypoxic ischemia, or a definite myelination delay. We also excluded abnormal findings outside the brain, such as a cephalic hematoma. By contrast, we did not exclude findings considered normal variations, such as transparent septal cysts. Additionally, scans with no abnormal findings in the required slices were not excluded even if there were abnormal findings in the remaining slices or if subjects had underlying neurological and neurodevelopmental disorders. The detailed information is provided in Table S1. A strong artifact was defined as one for which an image could not be clinically assessed. One investigator (MK), a pediatric neurologist who has radiological training, assessed all eligible 558 scans from the 441 subjects. The presence or absence of abnormal findings or a myelination delay in the required slice was assessed based on clinical reports by a pediatric radiologist. Finally, 187 MR scans from 161 subjects (dataset 1) were used as the training and test set for the deep learning model (Fig. 2).

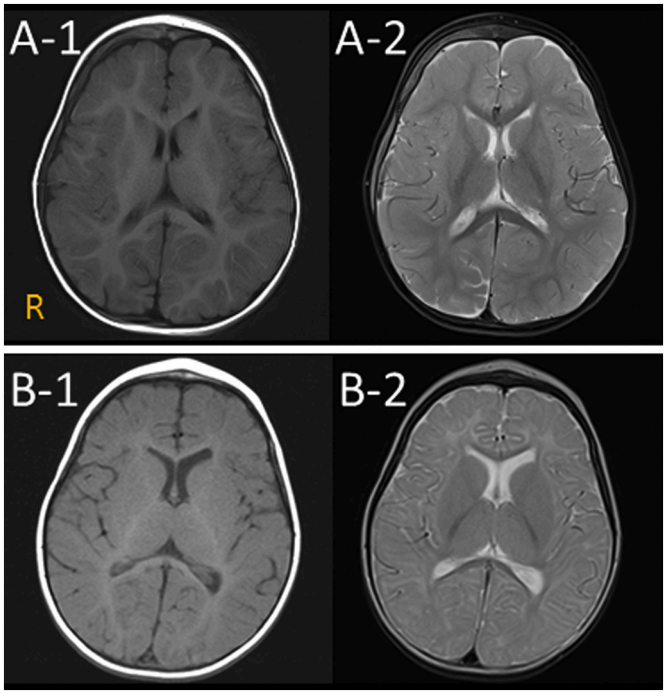

Fig. 1. Representative images from the datasets.
T1-(A1) and T2-(A2) weighted images of a 12-month-old subject included in dataset 1 and a 12-month-old subject included in dataset 2 (B1 and B2).

2.1.2. Dataset 2

Additionally, we collected brain MR images exhibiting a myelination delay in children aged 0–24 months acquired in our department. The following scans were included: 1) scans exhibiting a myelination delay, 2) scans that included the required axial slices of the T1w and T2w images, 3) scans of subjects who were not born preterm (gestational age < 37 weeks), and 4) scans without gross abnormal findings or strong artifacts. In dataset 2, we did not exclude MR images with subtle abnormal findings in addition to a myelination delay, because MR images with a myelination delay alone were rare. Finally, seven scans from six subjects were collected as dataset 2. One of the six patients was performed MR image scans twice at different age. The selection criteria for the imaging sequence and the required slices were the same as those described for dataset 1. The same investigator assessed the images in the same way. Representative T1w and T2w images from dataset 2 are shown in Fig. 1B1 and B2, respectively.

All MR images were acquired with one of the seven different 1.5 T or 3 T MR imaging scanners located in our hospital. The imaging parameters were roughly determined for each machine, and the imaging protocol was modified by the radiology technician according to the clinical needs. The scanner model, general imaging parameters, and the number of scans taken with each scanner are listed in Table S2.

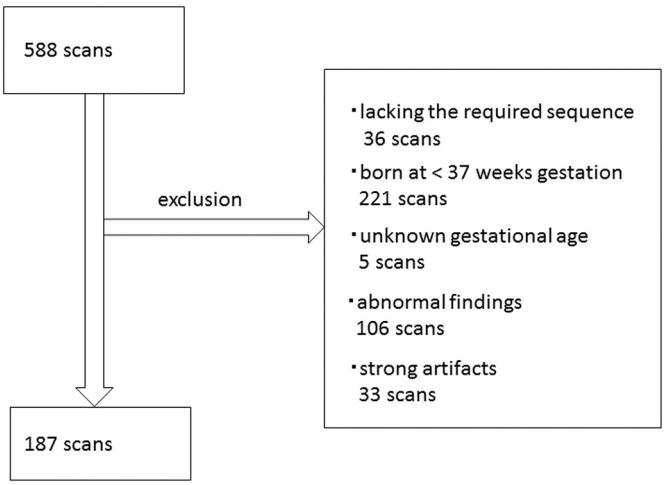

Fig. 2. Image inclusion and exclusion process flow for dataset 1.

2.2. Data processing

The original 2D axial images in both datasets were preprocessed. Initially, the acquired images were converted from DICOM to JPG format. Subsequently, the margins of the images were cropped at the outer surface of the brain to fit a square. Finally, the image was scaled to 128 × 128 pixels. Hence, the preprocessed imaging data contained not only cerebral parenchyma but also extracerebral structures, such as bone, subcutaneous tissue, and extra-axial cerebrospinal fluid (Fig. 1).

2.3. Training and testing the deep learning model

Deep learning models were developed using the commercially available software Neural Network Console® (Sony Network Communications Inc., Tokyo, Japan). Fig. 3 shows the network architecture of our CNN with four convolution layers. This in-house model processed T1w and T2w images in parallel, concatenated them in a further processing step, and then estimated brain age using linear regression. The scans in dataset 1 were divided randomly into the training (60%), validation (20%), and testing (20%) datasets (Fig. S1). These subsets were stratified by age group (0, 1–6, 7–12, 13–18, and 19–24 months). Each dataset contained 37 or 38 scans (the testing dataset included 37 scans). Age at the time of imaging was measured in weeks and used as a label. The learning parameters were a max epoch of 200 and a batch size of 19; the optimizer selected was Adam (α: 0.001, β: 0.9) [5].

2.4. Age estimates and statistical analysis

We performed four-fold cross-validation (Fig. S1). The final result of the AI model is the average of the estimates of the four models created during cross-validation. The MAE, root mean square error (RMSE), and Pearson's correlation coefficient (PCC) were calculated for the final result. When we compared the results of the AI model with those of human assessors, MAE and RMSE were converted from weeks to months. In addition, three human assessors (TS, HY, and HK) independently estimated brain ages in months from all images in test subset and were

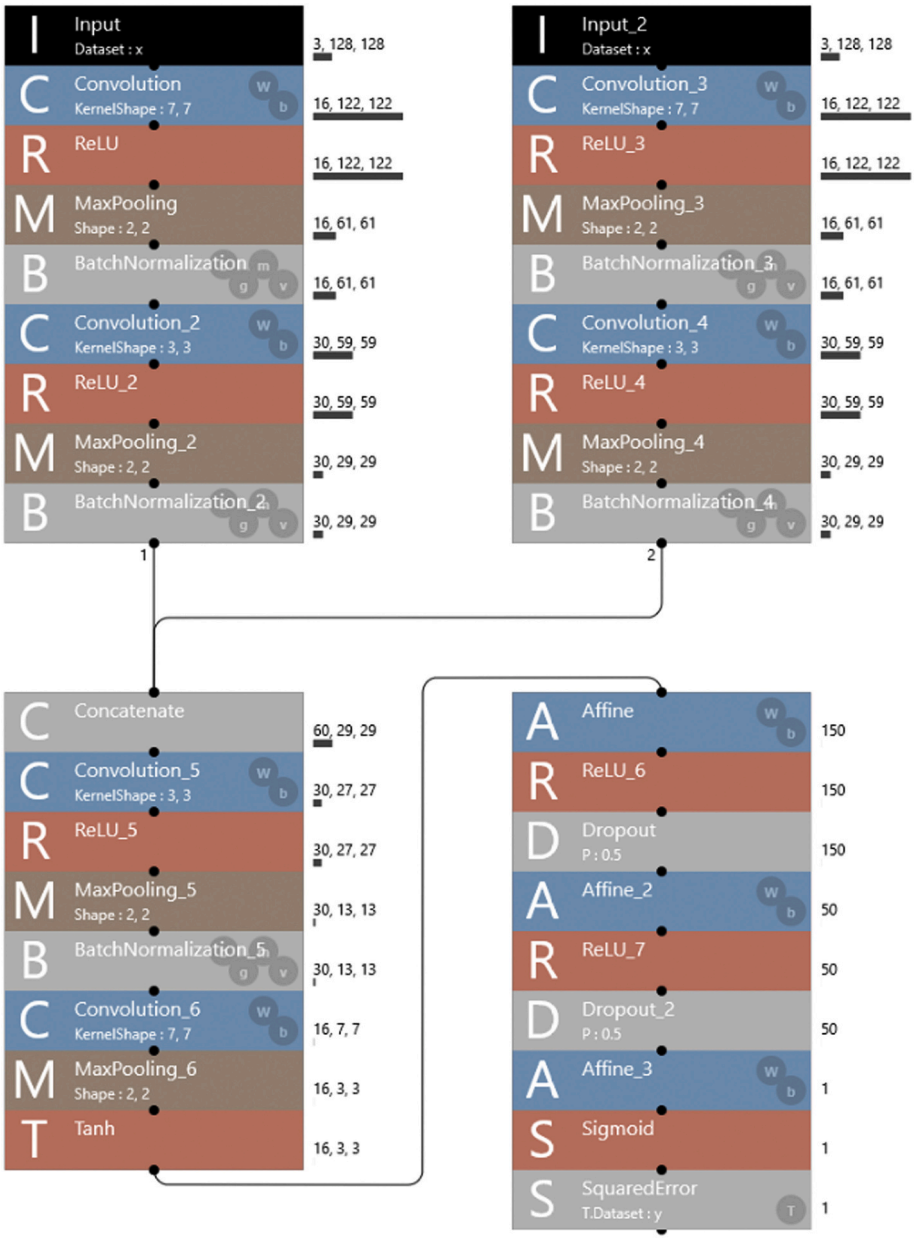

Fig. 3. The architecture of the convolutional neural network used in this study.

blinded to any of the clinical data. The assessors were Japanese pediatric neurologists who each had 10–23 years of radiological training in terms of assessing infant MR images. The mean of their estimates was used to represent the human specialist-derived age. The Wilcoxon signed-rank test was used to compare the estimates between the AI model and the human assessors. An F-test was used to compare the variance of the error between the AI model and human assessors. Additionally, a Bland-Altman analysis [6] was used to assess the agreement between the AI model and the assessors. In this analysis, the 95% limit of agreement (LOA) was defined as the mean ± two standard deviations (SDs), using the mean and SD of the difference between the estimates of the AI model and assessors. We defined an acceptable LOA range as one that is shorter than 3 months.

2.5. Age estimates using dataset 2

We performed brain age estimates of dataset 2 with the AI model. The three assessors also estimated brain ages from the images in dataset 2. The Wilcoxon signed-rank test was used to evaluate the consistency between estimated brain age and chronological age in the AI model.

Statistical analyses were performed with SPSS version 26 software (IBM Corp., Armonk, NY, USA). A p-value <0.05 was considered to denote significance.

2.6. Ethical review

This study was approved by the Ethics Review Committee of Nagoya University Graduate School of Medicine.

3. Results

3.1. Subjects

Of the 187 scans in dataset 1, 109 (58%) were obtained from male subjects and 78 (42%) from female subjects. Fig. 4 shows the distribution of chronological age at the time of the MR image scan. The largest group comprised newborn infants admitted to our neonatal intensive care unit ($n = 55$). Of the 187 scans, 162 (87%) were acquired by one of the 3-T MR imaging machines, and 25 (13%) were acquired by one of the 1.5-T machines (Table S2).

3.2. Training the deep learning model

Training was conducted without any problems. A representative learning curve for the cross-validations is shown in Fig. S2.

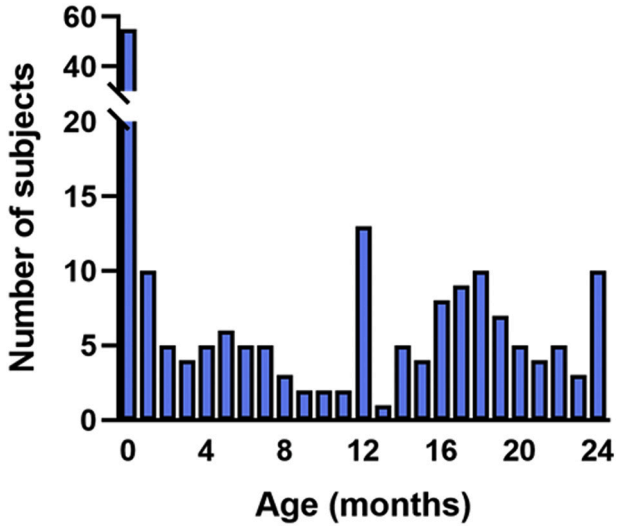

Fig. 4. Age distribution of the subjects in dataset 1.

3.3. Age estimates

The results of the age estimates from the AI model and three human assessors are summarized in Table 1. The MAE and RMSE of the AI model were 8.2 weeks (1.9 months) and 12.6 weeks (2.9 months), respectively. The PCC for the AI model was 0.94, showing a high correlation between chronological and estimated ages. All human assessors were also associated with high PCCs. No significant differences were observed between the estimates from the AI model and the mean estimates of the human assessors with the Wilcoxon signed-rank test ($p = 0.23$). Fig. 5 shows a scatter plot of the results from the AI model and the mean estimates of the human assessors. The 95% LOAs were larger than the pre-defined range for any of the assessors or the mean estimates of the assessors (Table 1). Thus, we did not observe a strong agreement between the AI model and the assessors.

Fig. 6 shows the distribution of the error between chronological age and the estimated age from the AI model or the mean of human assessors. The variance of the error was significantly larger for the AI model than the human assessors ($p < 0.001$). In the AI model, there were two outliers based on the threshold of the mean ± 2 SD. These two outliers, of 17.7 and 13.8 months, corresponded to chronological ages of 11 and 24 months, respectively. There is no specific cause of the large errors in images (Fig. S3), MR scanners used and acquisition parameters.

3.4. Age estimates of subjects with myelination delay

Clinical information about dataset 2, the age estimates from the AI model, and the mean estimates of the human assessors are shown in Table 2. The AI model estimated brain age to be younger than chronological age in all but one of the seven scans. A significant difference was observed between brain age estimated by the AI model and chronological age ($p = 0.028$).

4. Discussion

We performed brain age estimates based on MR images from children younger than 2 years of age using deep learning. Our AI model estimated brain age with a MAE of 8.2 weeks (1.9 months). The estimates of the AI model and human assessors did not satisfy the definition of agreement for Bland–Altman analysis, but the Wilcoxon signed-rank test showed no significant difference between their mean results. The AI model also estimated the brain ages of subjects with a myelination delay to be significantly younger than their chronological ages. These results indicate that the prediction accuracy of our AI model approached that of the human specialists and that our simple method with minimal preprocessing of clinical data can facilitate radiological assessment of brain

Table 1
The validity of the age estimates from the artificial intelligence (AI) models and human assessors.

Measurements	AI model	Human			
		assessor 1	assessor 2	assessor 3	mean of assessors
MAE (months)	1.9 (8.2 weeks)	1.2	1.5	1.2	1.1
RMSE (months)	2.9 (12.9 weeks)	1.7	2.3	2.0	1.5
PCC	0.94	0.98	0.98	0.98	0.98
95% LOA[a]	NA	0.63 ± 5.9	−0.06 ± 3.3	−1.09 ± 3.8	0.55 ± 4.7

MAE: mean absolute error, RMSE: root mean square error, PCC: Pearson's product-moment correlation coefficient, LOA: limit of agreement, NA: not applicable.

[a] Bland-Altman analysis.

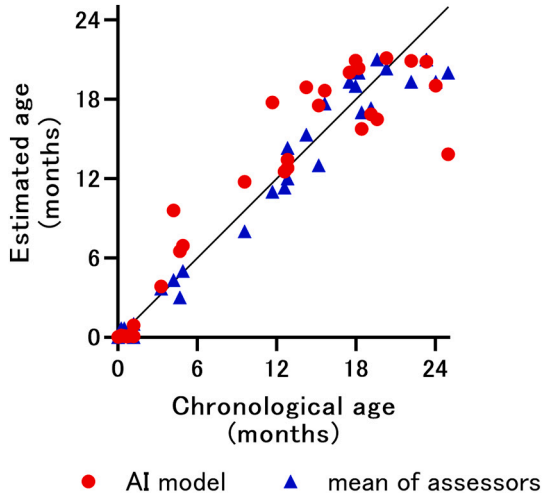

Fig. 5. Scatter plot of the estimates from the artificial intelligence (AI) model and mean estimates of the human assessors based on the test subset.
The line in the graph represents the ideal estimates. Red circles represent the results from AI model, and blue triangles represent those in the mean of the human assessors. (For interpretation of the references to colour in this figure legend, the reader is referred to the web version of this article.)

development and maturational changes in myelination.

Studies on age estimates based on brain MR images have increased exponentially, but the majority have evaluated adult subjects. Several investigations have been conducted on children and adolescent groups [7–13], but there are only a few reports on children younger than 2 years of age. Hu et al. performed age estimates of early infants aged 14–797 days [14]. They analyzed eight morphological features, such as cortical thickness and surface area, in 251 longitudinal scans to train their model, which combined a two-step prediction method with a complementary one-step prediction method, and the MAE was 32.1 days. They improved their accuracy by using multiple features and special models, but the data processing was complex. By contrast, we focused on the differences in MR images between infants and older age groups using myelination as observed in infant MR images as an indicator for age. Human specialists estimate brain ages from infant MR images according to myelination, and their work is clinically important for assessing brain maturation and diagnosing neurological diseases. Our AI model was created using a simple method, based on the way human specialists estimate brain age. Indeed, the model estimated brain age with a MAE of 1.9 months, which was close to that of the human specialists. A margin of error of 1.9 months was considered clinically acceptable.

Various imaging features have been used to estimate age. Most investigators pre-processed 3D T1w images and extracted specific features, then inputted them into machine learning. For example, Lewis et al. used 3D T1w intensity contrast between the GM and WM and cortical thickness [12]. Bermudez et al. combined two sets of features from 3D T1w MR images, such as intensity-derived features and volumetric features, using multi-atlas segmentation [15]. However, 3D T1w imaging is not yet routine clinical practice. On the other hand, conventional 2D T1w imaging is used in clinical practice because it provides a clear picture of brain structures, whereas T2w imaging is used to assess the presence of edema and inflammation. In the present study, we used a combination of T1w and T2w imaging because myelination as reflected by both T1w and T2w image contrasts can be observed in infant MR images. Also, we used only one axial slice of each of the raw T1w and

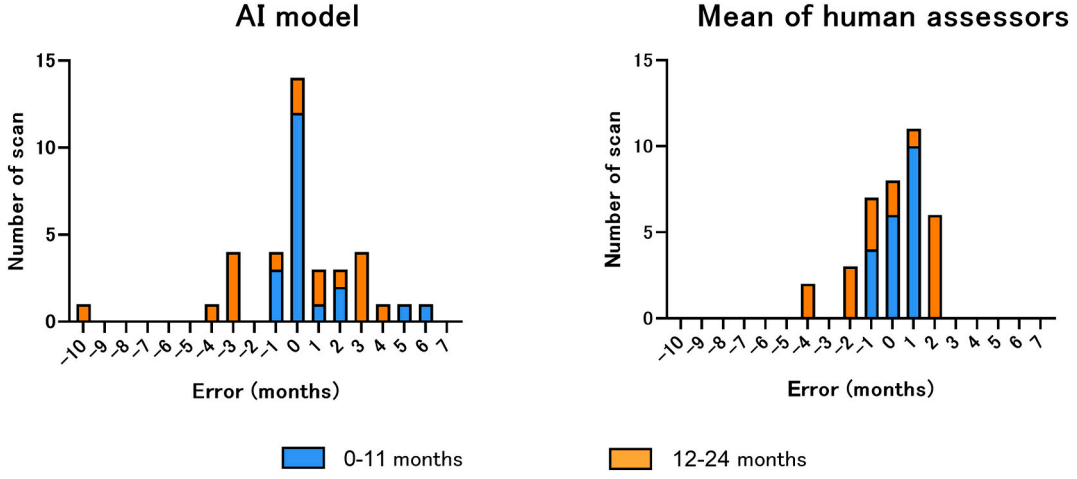

Fig. 6. Distribution of the error between chronological age and estimated age from the AI model (A) and the mean of human assessors (B).
Orange bars indicate the errors from the subjects aged 12–24 months, and blue bars indicate those from the subjects aged 0–12 months. (For interpretation of the references to colour in this figure legend, the reader is referred to the web version of this article.)

Table 2
Clinical characteristics and the age estimates of dataset 2.

Subjects	Sex	Diagnosis	Other MRI findings	Chronological age (month)	Estimated age (month)	
					AI model	Mean of assessors
1	F	Unknown	Hypoplasia of genu of corpus callosum	7.7	3.6	5.3
2	F	Gyrus dysplasia	Thinning of corpus callosum	7.9	7.9	3.7
				18.4	13.1	4.3
3	F	BPAN	None	12.4	6.3	7.0
4	M	Neonatal HIE	None	17.6	7.4	12.0
5	F	Congenital cerebral hypomyelination	None	20.9	5.9	5.0
6	F	BPAN	None	21.7	13.8	11.7

AI: artificial intelligence, HIE: hypoxic-ischemic encephalopathy, BPAN: β-propeller protein-associated neurodegeneration, F: female, M: male.

T2w images because we wanted to obtain an accurate estimate using the minimum amount of data for each subject, so that the method can also be applied in cases with scant data. This approach may be less informative than using whole-brain images. Nevertheless, our method has the advantage of immediate implementation in various clinical practices.

In this study, after excluding the two outliers, the MAE, RMSE, and PCC improved greatly to 1.4 months, 2.0 months, and 0.97, respectively. This indicates that the outliers had a large impact on the results. Understanding the reasons for large errors is important for improving the accuracy of AI models and achieving agreement with results of human specialists. Although we could not identify any specific cause of the large errors in images and acquisition parameters (Fig. S3), one possible reason is that the ages of the subjects in dataset 1 were skewed towards 0 months. The number of older subjects in the training dataset might have been insufficient. Another reason is that myelination was closer to completion in the scans of subjects older than 12 months, and the changes became smaller. Therefore, older subjects might be difficult to distinguish between ages. To overcome these issues, the number of subjects and distribution of ages in the dataset should be improved.

The deep learning model used in this study provided clinical utility for assessing myelination delay. The model estimated brain age to be younger than chronological age in all but one subject with delayed myelination. It is a major challenge to clarify the decision process of a deep learning model. Age estimates of adult brains using an AI model can be based on age-related brain atrophy [1], although evidence remains scarce. Bermudez et al. evaluated their AI model for brain age estimates using gradient-weighted class activation mapping (grad-CAM), which visualizes the region activated when an AI model is used [15,16]. They reported that head size, cerebral cortex, and size of the ventricles are activated with grad-CAM. In the current study, head size would not have been a factor because we cropped the margins and fit each image to a particular size before training. Our model estimated age from most of the scans with delayed myelination as younger than the chronological age. Therefore, it seems that our AI model predicted brain age based on contrast intensity of the GM and WM (i.e., myelination), although we cannot exclude the effect of other findings, such as gyrification, brain shape, and/or extra-cerebral structures.

The large gap between estimated brain age and chronological age offers a clue for recognizing deterioration in health. Cole et al. reported that older adults with a higher estimated brain age than their chronological age have a greater risk of death and poor physical and cognitive fitness [17]. It has also been reported that some disorders, such as Alzheimer's disease, schizophrenia, depression, mild cognitive impairment, epilepsy, Down syndrome, and traumatic brain injury, are associated with increased estimated brain age [18]. In this study, we revealed that infants with a lower estimated age compared to their chronological age had a risk of delayed myelination. Further studies are needed to elucidate the relationship between MR image findings other than myelination delay and the estimated age of infants.

This study had some limitations. First, we included images of subjects with underlying diseases and no abnormal findings in deep learning in this study. These images may include some subtle findings that we could not detect visually, which might have affected the analysis. Second, performing MR imaging on infants is often difficult without sedation. Therefore, there are few opportunities to perform MR scans on healthy infants who do not need it clinically. A public MR image database of healthy children is required. Third, we used only single-center data for training and testing the deep learning model. Data from multiple facilities should be used to assess the accuracy of the deep learning model [19]. However, we collected images acquired by seven different MR imaging scanners in our hospital. The field of strength and imaging parameters differed among them. Therefore, we created a situation similar to that of a multicenter study.

5. Conclusion

We performed brain age estimates using brain MR images of children younger than 2 years of age with deep learning. Although our AI model, characterized by a simple methodology and minimal requirement for raw MR image data, did not satisfy the definition of the agreement with human specialists, the accuracy of the brain age estimations was similar to that of human specialists. The brain age of subjects with a myelination delay was estimated to be younger than their chronological age. This is an important clinical indication for deep learning to estimate brain age objectively in this age group, particularly by non-specialists. Further studies are needed to improve accuracy, reduce outliers, and adapt the model to various medical conditions, including myelination delay.

Declaration of competing interest

The authors have no conflicts of interest to disclose.

Acknowledgments

We thank the radiology technicians for performing the MR imaging. We also thank the clinical radiologists for writing the interpretation reports. This research did not receive any specific grant from funding agencies in the public, commercial, or not-for-profit sectors.

Appendix A. Supplementary data

Supplementary data to this article can be found online at https://doi.org/10.1016/j.mri.2021.03.004.

References

[1] Sajedi H, Pardakhti N. Age prediction based on brain MRI image: a survey. J Med Syst 2019;43:279. https://doi.org/10.1007/s10916-019-1401-7.
[2] Franke K, Ziegler G, Klöppel S, Gaser C, The Alzheimer's Disease Neuroimaging Initiative. Estimating the age of healthy subjects from T1-weighted MRI scans using kernel methods: exploring the influence of various parameters. Neuroimage 2010; 50:883–92. https://doi.org/10.1016/j.neuroimage.2010.01.005.
[3] Greenspan H, Ginneken BV, Summers RM. Guest editorial deep learning in medical imaging: overview and future promise of an exciting new technique. IEEE Trans Med Imaging 2016;35:1153–9. https://doi.org/10.1109/TMI.2016.2553401.
[4] Barkovich AJ, Mukherjee P. Normal development of the neonatal and infant brain, skull, and spine. In: Barkovich AJ, Raybaud C, editors. Pediatric Neuroimaging. 5th ed. Philadelphia: Lippincott Williams & Wilkins; 2012. p. 20–80.
[5] Kingma DP, Ba JL. Adam: a method for stochastic optimization. http://arxiv.org/abs/1412.6980;; 2017.
[6] Bland JM, Altman DG. Statistical methods for assessing agreement between two methods of clinical measurement. Lancet 1986;1:307–10.
[7] Brown TT, Kuperman JM, Chung Y, Erhart M, McCabe C, Hagler Jr DJ, et al. Neuroanatomical assessment of biological maturity. Curr Biol 2012;22:1693–8. https://doi.org/10.1016/j.cub.2012.07.002.
[8] Cao B, Mwangi B, Hasan KM, Selvaraj S, Zeni CP, Zunta-Soares GB, et al. Development and validation of a brain maturation index using longitudinal neuroanatomical scans. Neuroimage 2015;117:311–8. https://doi.org/10.1016/j.neuroimage.2015.05.071.
[9] Erus G, Battapady H, Satterthwaite TD, Hakonarson H, Gur RE, Davatzikos C, et al. Imaging patterns of brain development and their relationship to cognition. Cereb Cortex 2015;25:1676–84. https://doi.org/10.1093/cercor/bht425.
[10] Franke K, Luders E, May A, Wilke M, Gaser C. Brain maturation: predicting individual BrainAGE in children and adolescents using structural MRI. Neuroimage 2012;63:1305–12. https://doi.org/10.1016/j.neuroimage.2012.08.001.
[11] Khundrakpam BS, Tohka J, Evans AC, Brain Development Cooperative Group. Prediction of brain maturity based on cortical thickness at different spatial resolutions. Neuroimage 2015;111:350–9. https://doi.org/10.1016/j.neuroimage.2015.02.046.
[12] Lewis JD, Evans AC, Tohka J, Brain Development Cooperative Group, the Pediatric Imaging, Neurocognition, and Genetics Study. T1 white/gray contrast as a predictor of chronological age, and an index of cognitive performance. Neuroimage 2018;173:341–50. https://doi.org/10.1016/j.neuroimage.2018.02.050.
[13] Wang J, Li W, Miao W, Dai D, Hua J, He H. Age estimation using cortical surface pattern combining thickness with curvatures. Med Biol Eng Comput 2014;52: 331–41. https://doi.org/10.1007/s11517-013-1131-9.
[14] Hu D, Wu Z, Lin W, Li G, Shen D. Hierarchical rough-to-fine model for infant age prediction based on cortical features. IEEE J Biomed Health Inform 2020;24: 214–25. https://doi.org/10.1109/JBHI.2019.2897020.

[15] Bermudez C, Plassard AJ, Chaganti S, Huo Y, Aboud KS, Cutting LE, et al. Anatomical context improves deep learning on the brain age estimation task. Magn Reson Imaging 2019;62:70–7. https://doi.org/10.1016/j.mri.2019.06.018.
[16] Selvaraju RR, Cogswell M, Das A, Vedantam R, Parikh D, Batra D. Grad-cam: visual explanations from deep networks via gradient-based localization. Proc IEEE Int Conf Comp Vision 2017:618–26. https://doi.org/10.1109/ICCV.2017.74.
[17] Cole JH, Ritchie SJ, Bastin ME, Valdés Hernández MC, Muñoz Maniega S, Royle N, et al. Brain age predicts mortality. Mol Psychiatry 2018;23:1385–92. https://doi.org/10.1038/mp.2017.62.
[18] Cole JH, Franke K. Predicting age using neuroimaging: innovative brain ageing biomarkers. Trends Neurosci 2017;40:681–90. https://doi.org/10.1016/j.tins.2017.10.001.
[19] Bluemke DA, Moy L, Bredella MA, Ertl-Wagner BB, Fowler KL, Goh VJ, et al. Assessing radiology research on artificial intelligence: a brief guide for authors, reviewers, and readers-from the radiology editorial board. Radiology 2020;294:487–9. https://doi.org/10.1148/radiol.2019192515.